PLOS ONE

RESEARCH ARTICLE

Chaos and multi-scroll attractors in RCL-shunted junction coupled Jerk circuit connected by memristor

Jun Ma[1,2]*, Ping Zhou[1], Bashir Ahmad[3], Guodong Ren[2], Chunni Wang[2]

1 School of Science, Chongqing University of Posts and Telecommunications, Chongqing, China, **2** Department of Physics, Lanzhou University of Technology, Lanzhou, China, **3** NAAM-Research Group, Department of Mathematics, King Abdulaziz University, Jeddah, Saudi Arabia

* hyperchaos@163.com

Citation: Ma J, Zhou P, Ahmad B, Ren G, Wang C (2018) Chaos and multi-scroll attractors in RCL-shunted junction coupled Jerk circuit connected by memristor. PLoS ONE 13(1): e0191120. https://doi.org/10.1371/journal.pone.0191120

Editor: Yongle Wu, Beijing University of Posts and Telecommunications, CHINA

Received: October 9, 2017

Accepted: December 28, 2017

Published: January 17, 2018

Data Availability Statement: All relevant data are within the paper and its Supporting Information files.

Funding: This project is supported by National Natural Science Foundation of China under Grant Nos. 11672122 and 11365014. The funders have no role in study design, data collection and analysis, decision to publish, or preparation of the manuscript.

Competing interests: The authors have declared that no competing interests exist.

Abstract

In this paper, a new four-variable dynamical system is proposed to set chaotic circuit composed of memristor and Josephson junction, and the dependence of chaotic behaviors on nonlinearity is investigated. A magnetic flux-controlled memristor is used to couple with the RCL-shunted junction circuit, and the dynamical behaviors can be modulated by changing the coupling intensity between the memristor and the RCL-shunted junction. Bifurcation diagram and Lyapunov exponent are calculated to confirm the emergence of chaos in the improved dynamical system. The outputs and dynamical behaviors can be controlled by the initial setting and external stimulus as well. As a result, chaos can be suppressed and spiking occurs in the sampled outputs under negative feedback, while applying positive feedback type via memristor can be effective to trigger chaos. Furthermore, it is found that the number of multi-attractors in the Jerk circuit can be modulated when memristor coupling is applied on the circuit. These results indicate that memristor coupling can be effective to control chaotic circuits and it is also useful to reproduce dynamical behaviors for neuronal activities.

Introduction

Chaos emergence can be observed in complex nonlinear systems [1–3]. In a practical way, nonlinear circuits [4–7] can generate chaotic series by setting appropriate parameters carefully, and it is believed that chaotic systems can be used for secure communication and image encryption [8–12]. Within the dimensionless dynamical models, nonlinearity is necessary for generating chaos and hyperchaos that one positive Lyapunov exponent at least can be detected in the sampled times for observable variables. Chaotic behaviors are often regarded as harmful and chaos should be suppressed; therefore, many schemes have been proposed to control the chaos [13–17]. Particularly, the author of this paper calculated the Hamilton energy [18] of dynamical system and suggested that energy modulation [19] can be used to control the dynamical states of hidden attractors. On the other hand, to keep consensus and realize synchronization, some chaotic systems are often used to investigate different kinds of

synchronization problems. For example, parameter estimation [20–23] based on synchronization is discussed, and thus self-adaptive control schemes are appreciated for reaching synchronization and control [24–27] on chaotic systems. In the case of chaos suppression and stabilization, uncertainty and control period should be considered. For example, *Mobayen et al.*[28,29] discussed the finite-time stabilization and second-order fast terminal sliding mode control design for chaotic systems with uncertainty, and the reliability of LMI approach has been confirmed. Furthermore, this scheme is carried out on synchronization problems even associated with fractional order dynamical system as well [30,31]. Indeed, the synchronization transition and control [32–35] on chaotic networks become more attractive because spatiotemporal systems show more complex dynamical behaviors than low-dimensional chaotic systems. All the nodes of the network used to keep pace with each other and the network becomes homogeneous state when complete synchronization is reached. Indeed, pattern formation and selection [36–42] could be another interesting aspect to investigate the collective behaviors of network. For example, spiral waves and Turing patterns can be induced and developed in biological networks, ecological systems and square array composed of coupled oscillators [43,44]. In fact, the self-organization and synchronization behaviors mainly depend on the local kinetics of nodes. Therefore, it is important to investigate the dynamics of isolated oscillators with different nonlinear properties, and it could be helpful for further investigation on collective behaviors of coupled oscillators and networks.

To enhance the complexity and nonlinearity, time delay is often introduced into some dynamical systems. For isolated oscillators, time delay can be thought as intrinsic, and it is often called as response time delay. For some interneurons, autapse[45,46], which is a specific synapse connects the axon and dendron or soma, introduces time delay along the close loop. As a result, the self-adaption of neuron to external forcing and stimulus is enhanced [47–49]. For example, appropriate distribution of autapse in the neuronal network can enhance the synchronization degree [50], and regular spatial patterns [51,52] can be developed. As argued by the author in Ref. [53], it is believed that the autapse formation could be associated with the injury on axon of neuron, thus an auxiliary loop is set up to help signal propagation and overcome the injured area. In setting of chaotic circuits, nonlinear electric devices such as negative resistor, nonlinear capacitor, and nonlinear inductor are critical to supply nonlinearity of the circuits. Josephson junction [54,55] is an important nonlinear inductor because of its sensitivity and superconductivity, and it plays important role in constructing chaotic circuits. For example, Josephson junction coupled resonator is used to simulate the electrical activities of neuron [53,56,57]. Particularly, a new electric device memristor [44,58,59], whose memductance is dependent on the inputs current, is often used to design various chaotic systems [60–62] for dynamical analysis and potential application for signal processing. It is confirmed that memristor-based circuit can show distinct memory effect because the memductance is fixed when external stimulus on memristor is moved. Due to its memory effect, the author of the paper suggested that memristor coupling and magnetic flux [63] can be used to describe the effect of electromagnetic induction and radiation in electrical activities of neurons [64–66]. Furthermore, memristor coupling is used to model the transition of electrical activities in cardiac tissue exposed to electromagnetic radiation, and the potential mechanism of heart disease induced by electromagnetic radiation is explained [67]. The improved neuronal circuits composed of memristors are used to investigate the synchronization behaviors [68], while extensive potential application of memristor keeps open.

In this paper, memristor is used to bridge a RCL-shunted junction circuit and the jerk circuit composed of infinite scroll attractors, thus an extended chaotic system can be formed for dynamical analysis and control. By changing the feedback gain in memristor on the coupled circuit, the infinite scroll attractors can be stabilized, and chaos can also be controlled.

Model setting and description

Due to the sensitive effect of electrical inductance, Josephson junction is often used to couple with resistor, capacitor, and inductor. As a result, a RCL-shunted circuit can be designed for potential analysis and synchronization application [69,70]. The circuit diagram is plotted in Fig 1.

According to the Kirchhoff's law, the circuit equations can be described as follows

$$\begin{cases} C\dfrac{dV}{dt} = I_{ext} - \dfrac{V}{R(V)} - I_c\sin(\gamma) - I_s - I_N \\ \dfrac{\hbar}{2e}\dfrac{d\gamma}{dt} = V \\ L\dfrac{dI_s}{dt} = V - I_sR_s - V_N \end{cases} ; \quad (1)$$

where I_s denotes the current flowing in the shunt branch, L and R_s is the shunt inductance and shunt resistance, respectively. I_N, V_N is the fluctuating current noise and voltage noise that are

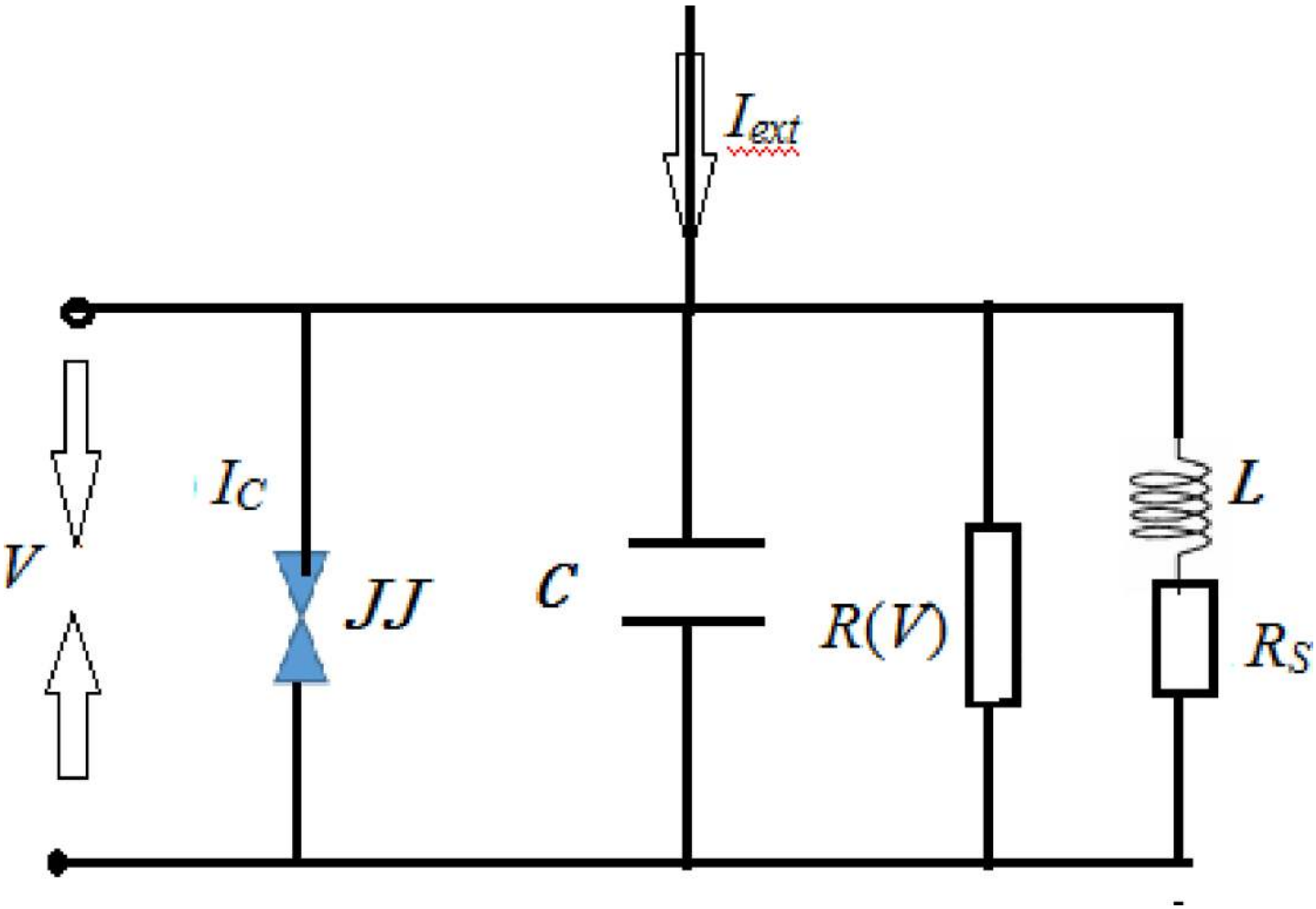

Fig 1. Diagram for RCL-shunted junction circuit. A Josephson junction is represented by three parallel channels, the supercurrent $I_c sin(\gamma)$, a capacitor C due to the overlap geometry, and a resistive channel modeling the quasiparticle leakage current. An inductance L followed with a shunt resistance R_s is used as a shunt branch.

https://doi.org/10.1371/journal.pone.0191120.g001

presented in the dissipative elements $R(V)$ and R_s, respectively. The parameter $\hbar$ represents Planck's constant, and C is the capacitance. As reported in Ref.[71], a voltage-dependent junction resistance is defined by

$$R(V) = \begin{cases} R_N & if|V| > V_g \\ R_{sg} & if|V| \leq V_g \end{cases} \tag{2}$$

A scale transformation is applied on Eq (1) to find a dimensionless dynamical system by using the following criterion.

$$\begin{cases} \tau = \omega_c t = t2eI_cR_s/\hbar; \beta_c = 2eI_cR^2{}_sC/\hbar; \beta_L = 2eI_cL/\hbar; i = I_{ext}/I_C; g = R_s/R(V); \\ x_1 = \gamma \bmod 2\pi; x_2 = V/I_cR_s; x_3 = I_s/I_c; \end{cases} \tag{3}$$

When the noise terms I_N, V_N are neglected, a shunted linear resistive-capacitive junction (RCLSJ) [70, 72] is described by

$$\begin{cases} \dot{x}_1 = x_2 \\ \dot{x}_2 = (i - g(x_2)x_2 - \sin x_1 - x_3)/\beta_C \\ \dot{x}_3 = (x_2 - x_3)/\beta_L \end{cases}; \tag{4}$$

$$g(x_2) = \begin{cases} 0.366 & |x_2| > 2.9 \\ 0.061 & |x_2| \leq 2.9 \end{cases}; \tag{5}$$

where the variable x_1, x_2, and x_3 often denotes the phase difference, junction voltage and current through the shunted inductance, respectively. The nonlinear function $g(x_2)$ measures the current-voltage relation between junction resistances in Eq (2). The parameter β_C, β_L, defines the capacitive, inductance constants, respectively. For more detailed description, readers can refer to Ref.[71] and references therein. As confirmed in Ref.[73], chaotic state can be detected when the parameters are fixed at $\beta_C = 0.707$, $\beta_L = 2.6$, and external forcing DC current $i = 1.2$. In fact, infinite equilibrium points are approached as $(n\pi, 0, 0)$ when external forcing current is removed, where n is integer and $n = 1, 2, 3, \ldots N$. Surely, bifurcation and linear stability analysis [74] could also be helpful to confirm the emergence of chaos in Josephson junction-coupled system. To enhance the nonlinearity and complexity, memirstor [75,76] is used for setting circuits which the outputs much depend on the initial setting for variables. For example, *Chua et al.* [76] presented a rigorous and comprehensive nonlinear circuit-theoretic foundation for the memristive Hodgkin-Huxley axon circuit model, which comprised a potassium ion-channel memristor and a sodium ion-channel memristor, along with some mundane circuit elements. It is known that the memductance of memristor is dependent on the inputs current, and the magnetic flux-dependent memristor is described by

$$\rho(\varphi) = \frac{dq(\varphi)}{dt} = \alpha + 3\beta\varphi^2 \tag{6}$$

where α, β are parameters associated with the memristor. Magnetic flux φ is used as a new variable in the improved dynamical system, and the memristor-coupled-Josephson Junction

system is described by

$$\begin{cases} \dot{x}_1 = x_2 \\ \dot{x}_2 = (i - g(x_2)x_2 - \sin x_1 - x_3)/\beta_C - k\rho(\varphi)x_2 \\ \dot{x}_3 = (x_2 - x_3)/\beta_L \\ \dot{\varphi} = kx_2 \end{cases}; \tag{7}$$

where the term kx_2 describes the effect of electromagnetic induction, and the term $k\rho(\varphi)x_2$ represents the induction current as follows

$$i' = \frac{dq}{dt} = \frac{dq}{d\varphi}\frac{d\varphi}{dt} = \rho(\varphi)V = k\rho(\varphi)x_2 \tag{8}$$

As a result, there are five bifurcation parameters (β_C, β_L, k, α, β) that can be adjusted to change the outputs and dynamical behaviors in Eq (7) except the input current. Make a contrast between Eq (4) and Eq (7), it is found that the modulation can keep certain symmetry in absence of external forcing as $i = 0$ by using the following transformation

$$(x_1, x_2, x_3, \varphi) \leftrightarrow (-x_1, -x_2, -x_3, -\varphi) \tag{9}$$

And the phase constraint is approached by

$$\nabla V = \frac{\partial \dot{x}_1}{\partial x_1} + \frac{\partial \dot{x}_2}{\partial x_2} + \frac{\partial \dot{x}_3}{\partial x_3} + \frac{\partial \dot{\varphi}}{\partial \varphi} = -g(x_2) - k\rho(\varphi) - 1/\beta_L \tag{10}$$

As shown in Eq (5), $-g(x_2)$ is always negative. As a result, the improved dynamical system shown in Eq (7) can be dissipative and it is consistent with the original dynamical system shown in Eq (4). In fact, negative dissipativity for dynamical system in the sense (10) may admits unbounded attractors because of existence of Jerk function. For better understanding the dissipativity in the sense of Levinsov (i.e. existence of convex absorbing set), readers can find useful guidance in Refs.[77,78]. In a dynamical view, chaos and even hyperchaos could be induced in Eq (7) by setting appropriate parameters. However, the attractor formation and orbit selection could be also dependent on the selection of initials setting when memristor coupling is used to control the RCL-shunted Junction circuit. Therefore, the outputs voltage x_2 (or

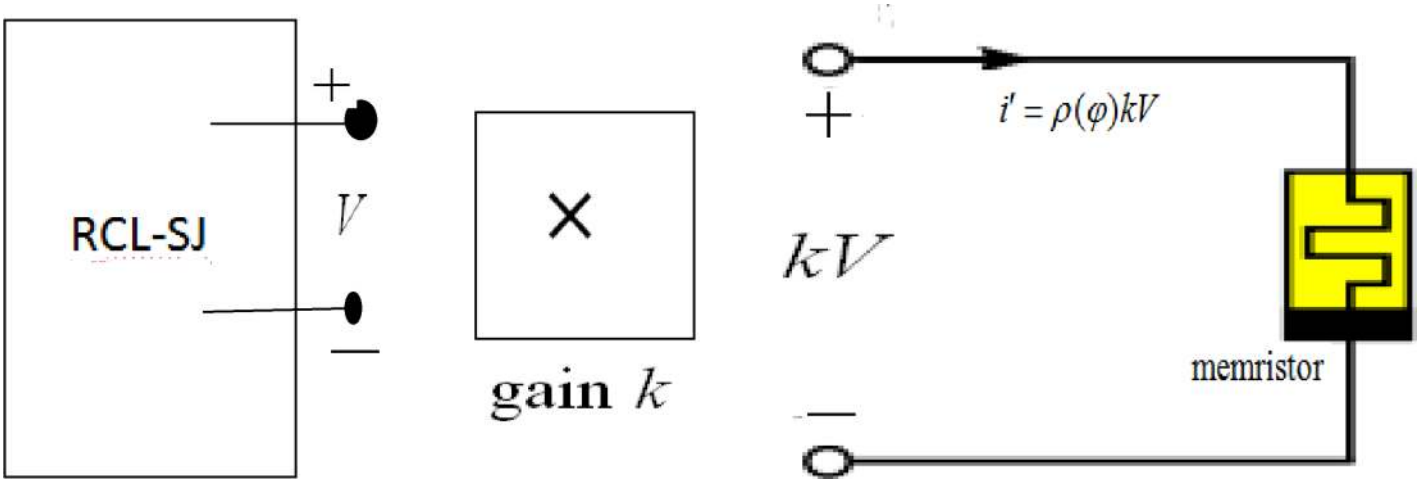

Fig 2. Schematic diagram for memristor-coupled RCL-SJ circuit.

https://doi.org/10.1371/journal.pone.0191120.g002

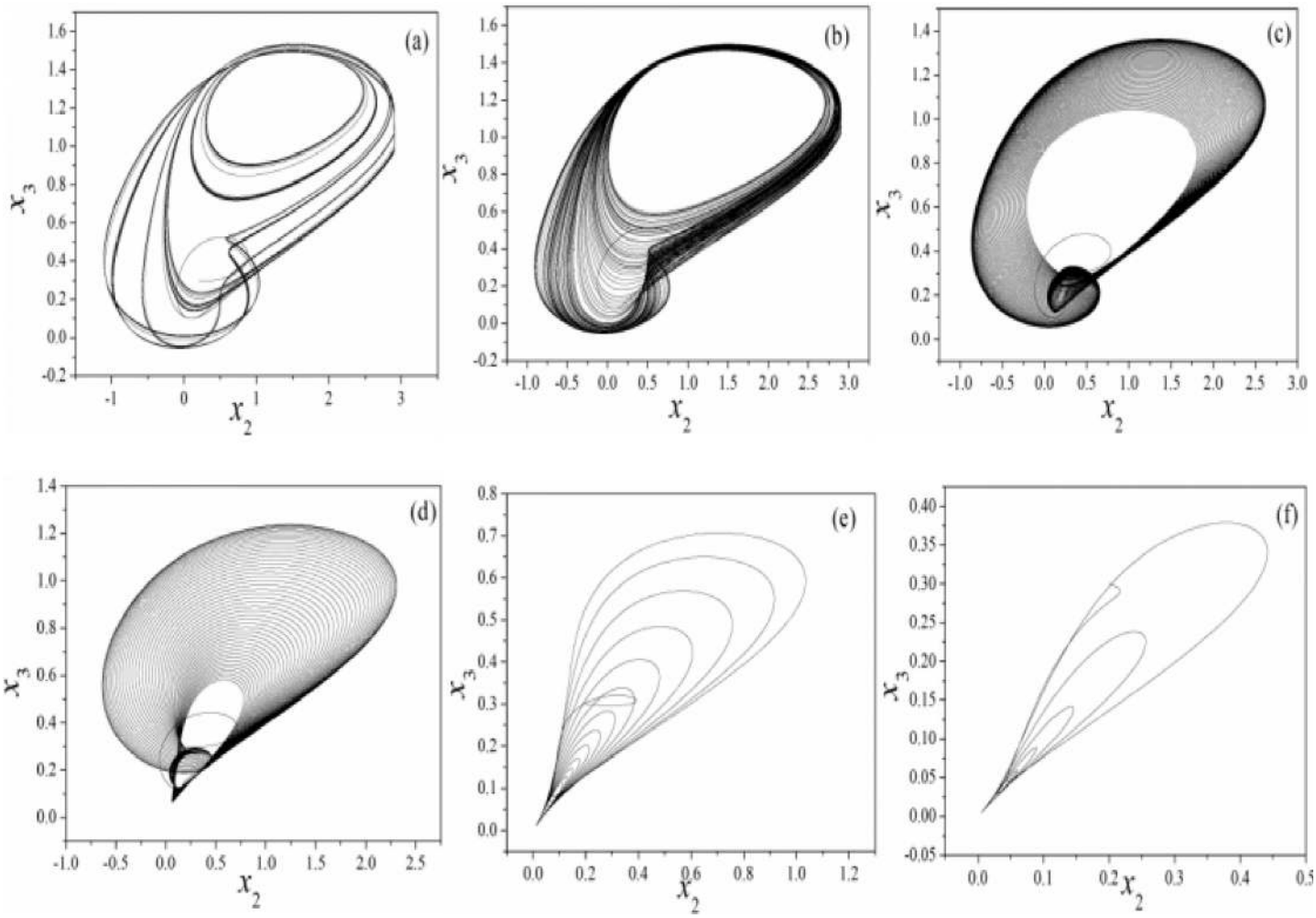

Fig 3. Phase portrait for variable (x_2 *vs.* x_3) is calculated by setting different feedback gains. (a)$k = 0$, (b)$k = 0.01$, (c)$k = 0.05$, (d)$k = 0.1$, (e)$k = 0.5$, (*f*)$k = 1.2$. The parameters in memristor are selected as $\alpha = 4$, $\beta = 0.01$, and calculating period is within 1500 time units.

https://doi.org/10.1371/journal.pone.0191120.g003

V) can be adjusted by appropriate gain k on the induction current contributed by a memristor, and the coupled circuit is shown as follows

According to Eq (7) and Fig 2, switch the feedback type (negative or positive) can suppress or enhance the chaotic behaviors in RCL-shunted circuit. In the next section, the Lyapunov exponents and phase portraits will be calculated for discussion and suggestion.

Numerical and experimental investigation

In this section, the fourth order Runge-Kutta algorithm is used to find solutions for Eq (7) with time step $h = 0.01$. For simplicity, $\beta_C = 0.707$, $\beta_L = 2.6$, and parameters k, α, β are carefully selected to investigate the electrical activities and dynamical behaviors. Furthermore, the Lyapunov exponent spectrum is calculated by changing the feedback gain k, and the effect of initial setting is also discussed. It is found that the improved Eq (7) can be reduced to the original Eq (4) by setting the coupling intensity as $k = 0$. That is to say, the effect of memristor is critical to induce transition of electrical activities from the outputs. For simplicity, at first, parameters α, β in the memristor are selected as $\alpha = 4$, $\beta = 0.01$, the external *DC* current $i = 1.2$. The phase

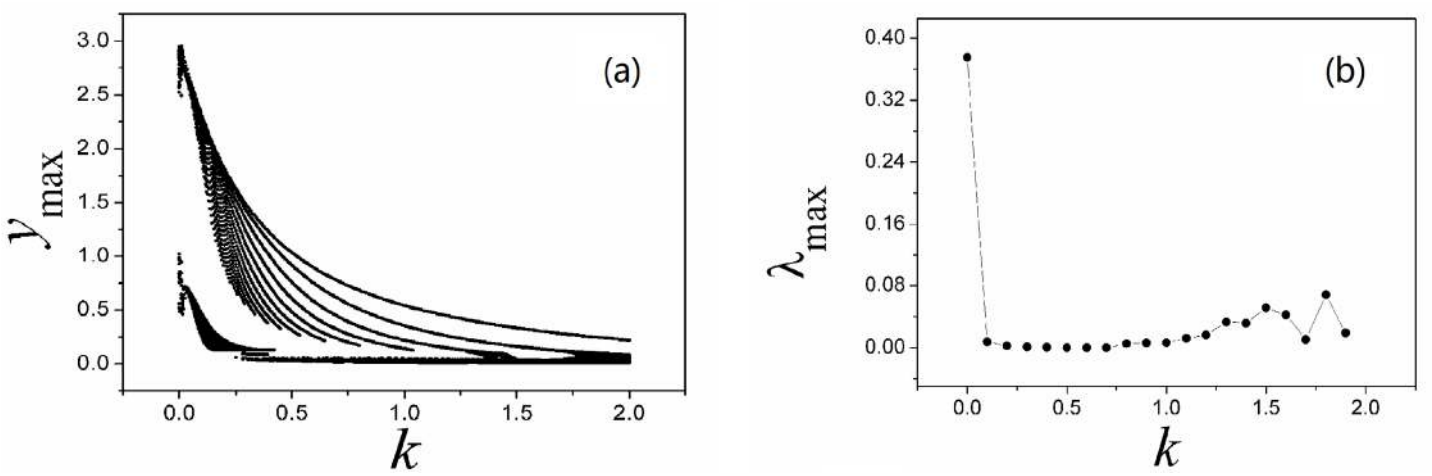

Fig 4. Bifurcation diagram (a) and Largest Lyapunov diagram (b) are calculated by changing the coefficient *k*. The parameters are selected as $\alpha = 4$, $\beta = 0.01$, $i = 1.2$, y_{max} is the maximal value of sampled time series for variable y.

https://doi.org/10.1371/journal.pone.0191120.g004

portraits are calculated by setting different feedback gains, and the initial values are selected as $(x_1(0), x_2(0), x_3(0), \varphi_0) = (0.1, 0.2, 0.3, 0)$.

It is found that the chaotic states are suppressed by further increasing the feedback gain k for memristor coupled by Josephson junction. According to Eq (4), the memristor can impose negative feedback on the junction voltage and thus the chaos can be controlled by setting larger feedback gains. However, the results in Fig 3B find that the orbits become more dense than the original RCLSJ shown in Eq (1) due to higher nonlinearity when the circuit is modulated by a memristor. Furthermore, the bifurcation analysis and the largest Lyapunov exponent are carried out in Fig 4.

The results in Fig 4 confirmed that the largest Lyapunov exponent and the maximal value for variable are decreased synchronously, the orbits become spare before reaching periodical states. In fact, in case of DC stimuli, it is more important to find spiking behavior by setting appropriate feedback gain, and the results are plotted in Fig 5.

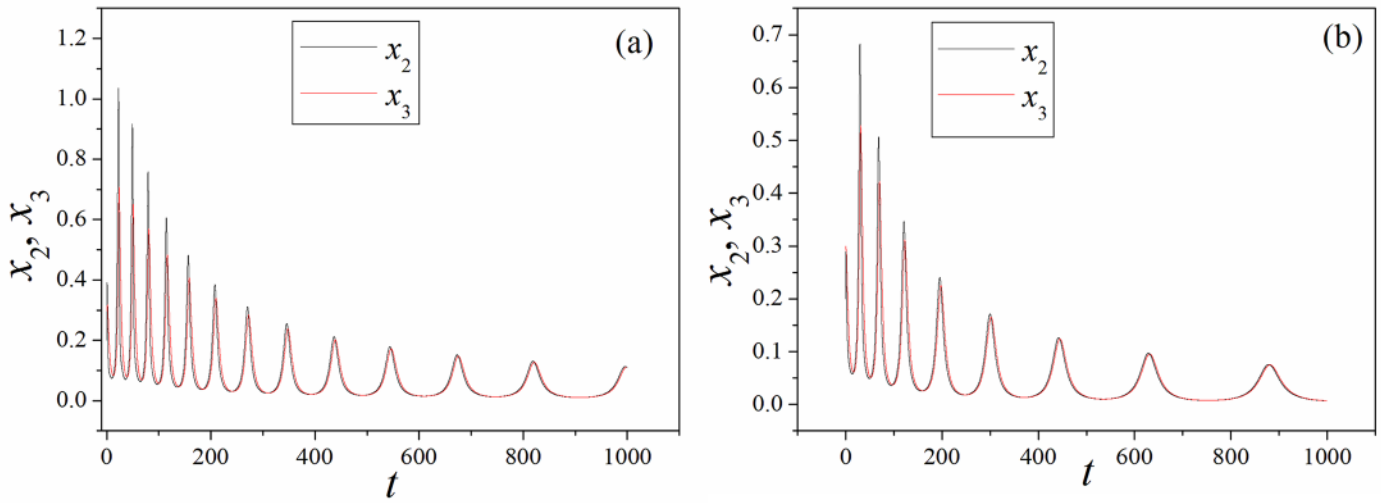

Fig 5. Sampled time series for junction voltage (x_2) and current (x_3). (a)$k = 0.5$, (b)$k = 0.8$. Parameters in memristor are selected as $\alpha = 4$, $\beta = 0.01$, $i = 1.2$.

https://doi.org/10.1371/journal.pone.0191120.g005

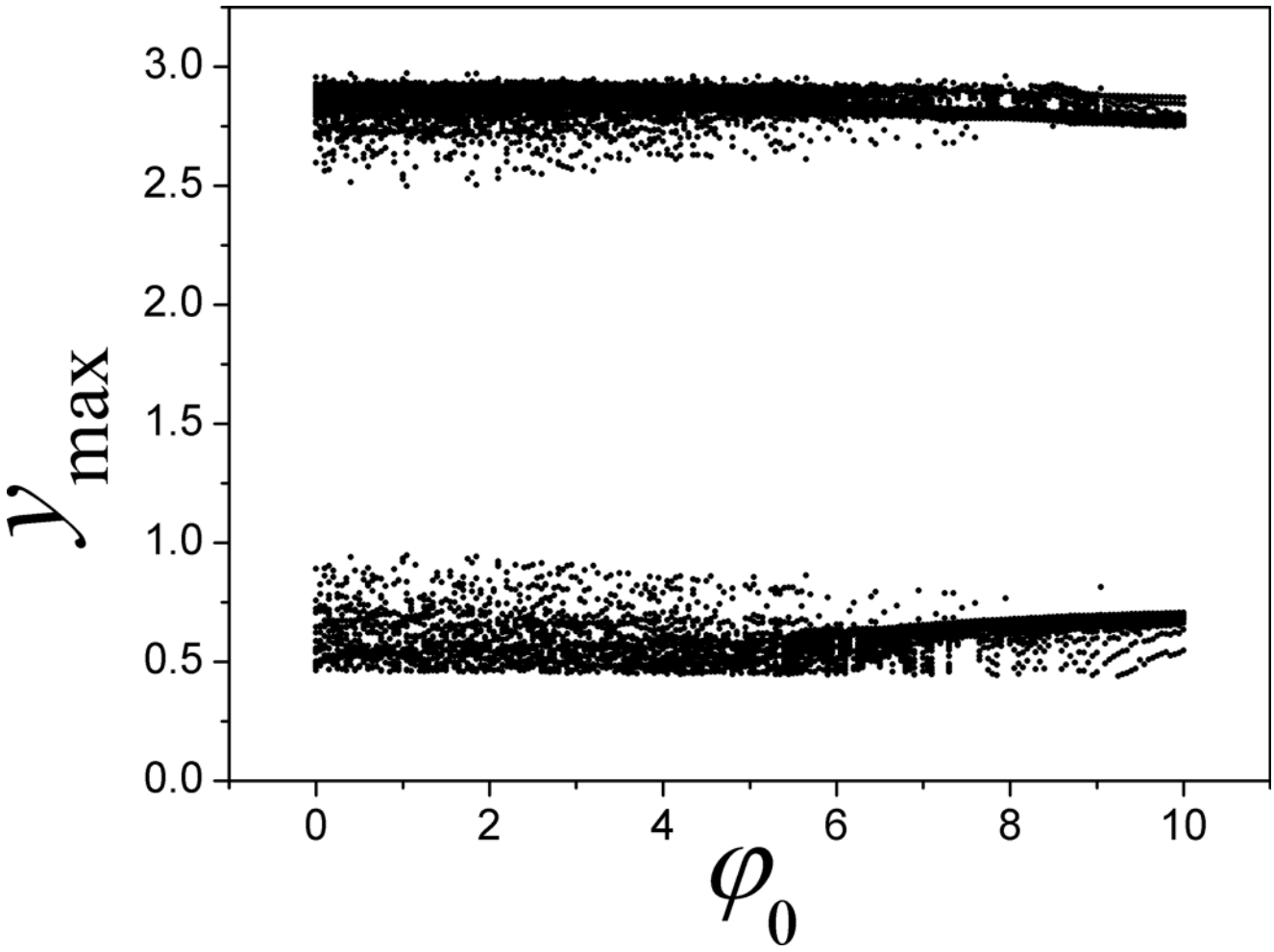

Fig 6. Bifurcation diagram is calculated for maximal state variable y_{max} vs the parameter φ_0. The parameters are selected as $\alpha = 4$, $\beta = 0.01$, $k = 0.01$.

https://doi.org/10.1371/journal.pone.0191120.g006

It is found in Fig 5 that the amplitude of junction voltage and current can be decreased by further increasing the feedback gain for memristor, and transient periodical oscillation can be observed in the sampled time series during the control of chaotic behaviors. Extensive numerical results are carried out by setting different initial values for variable φ. In Fig 6, the dependence of initial setting for magnetic flux in Eq (7) is calculated.

It is confirmed that the outputs and attractors are much dependent on the initial setting, as a result, switch and resetting the initial value for magnetic flux can trigger different attractors even other parameters are fixed.

However, in the case of negative feedback type, the results seem to be independent of the initials setting completely, and it is some different from the initial-dependent nonlinear system that the developed attractors are much dependent on the initial setting [79]. The potential mechanism could be that the magnetic flux is mainly dependent on junction voltage while it is independent of other variables. In fact, the dynamical behaviors in Eq (7) are also dependent on the external DC stimuli. Therefore, the Lyapunov exponent spectrum is calculated by changing the DC stimuli, and then the feedback gain is also changed to detect the transition of electrical activities at fixed DC stimuli. Furthermore, another group of parameters are setting to investigate the sampled time series and transition of attractors, the results are plotted in Fig 7.

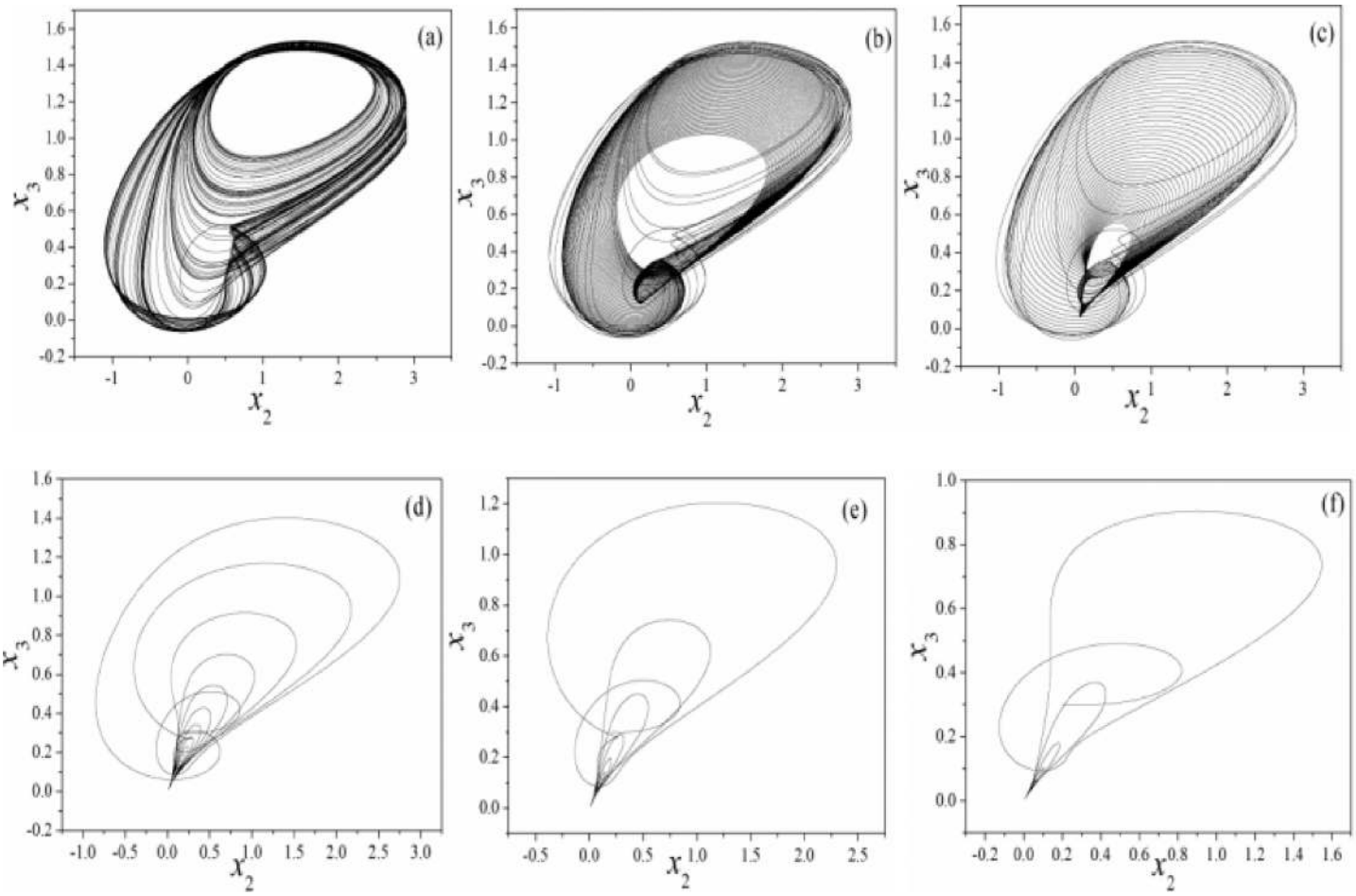

Fig 7. Phase portrait for variable (x_2 *vs.* x_3) is calculated by setting different feedback gain within 1500 time units. (a)$k = 0.01$, (b)$k = 0.05$, (c)$k = 0.1$, (d)$k = 0.5$, (e) $k = 0.8$, (*f*)$k = 1.2$. Parameters in memristor are selected as $\alpha = 0.1$, $\beta = 0.01$.

https://doi.org/10.1371/journal.pone.0191120.g007

With a contrast the results in Fig 3 and Fig 7, it is found that the formed attractors are dependent on the parameters in memristor, and a larger parameter setting for α can be more effective to suppress chaos and generate periodical behaviors in the outputs. Also, the bifurcation analysis and largerst Lyapunov exponent are further calculated for verification, and the results are shown in Fig 8.

Smaller value for parameters α, β can decrease the effect of induction current, while increase of feedback intensity k can enhance the negative feedback contribution, as a result, the dynamical behaviors are suppressed. The results in Fig 8 found that the largest Lyapunov exponent and maximal value for variables are decreased with increasing the feedback gain. It is also important to investigate the case when external stimuli and also feedback gain k are set under a larger value, and the distribution for Lyapunov exponent spectrum is calculated in Fig 9.

The results in Fig 9 found that appropriate external stimuli is helpful to support the emergence of chaos, then the chaos is removed by further increasing the external DC stimuli. When the effect of memristor is enhanced by increasing the feedback gain k, the chaotic behavior can be suppressed and even removed. The potential mechanism is that larger coupling intensity between memristor and RCL-shunted junction can input larger forcing current into the

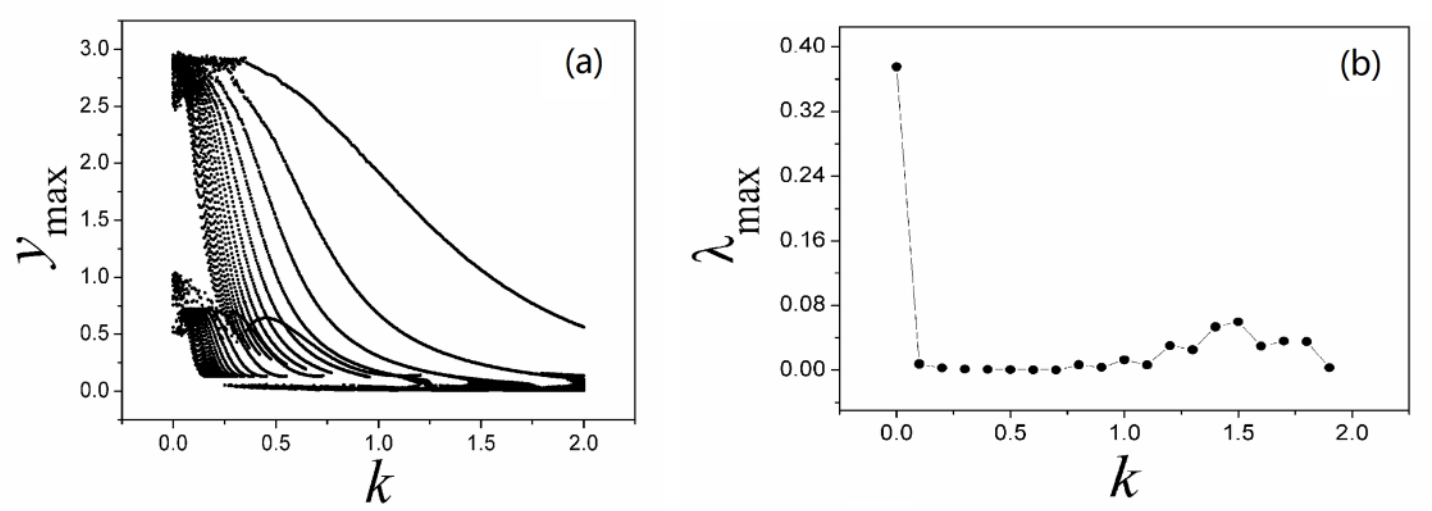

Fig 8. Bifurcation diagram (a) and Largest Lyapunov diagram (b) are calculated by changing the coefficient *k*. The parameters are selected as $\alpha = 0.1$, $\beta = 0.01$, $i = 1.2$, y_{max} is the maximal value of sampled time series for variable y.

https://doi.org/10.1371/journal.pone.0191120.g008

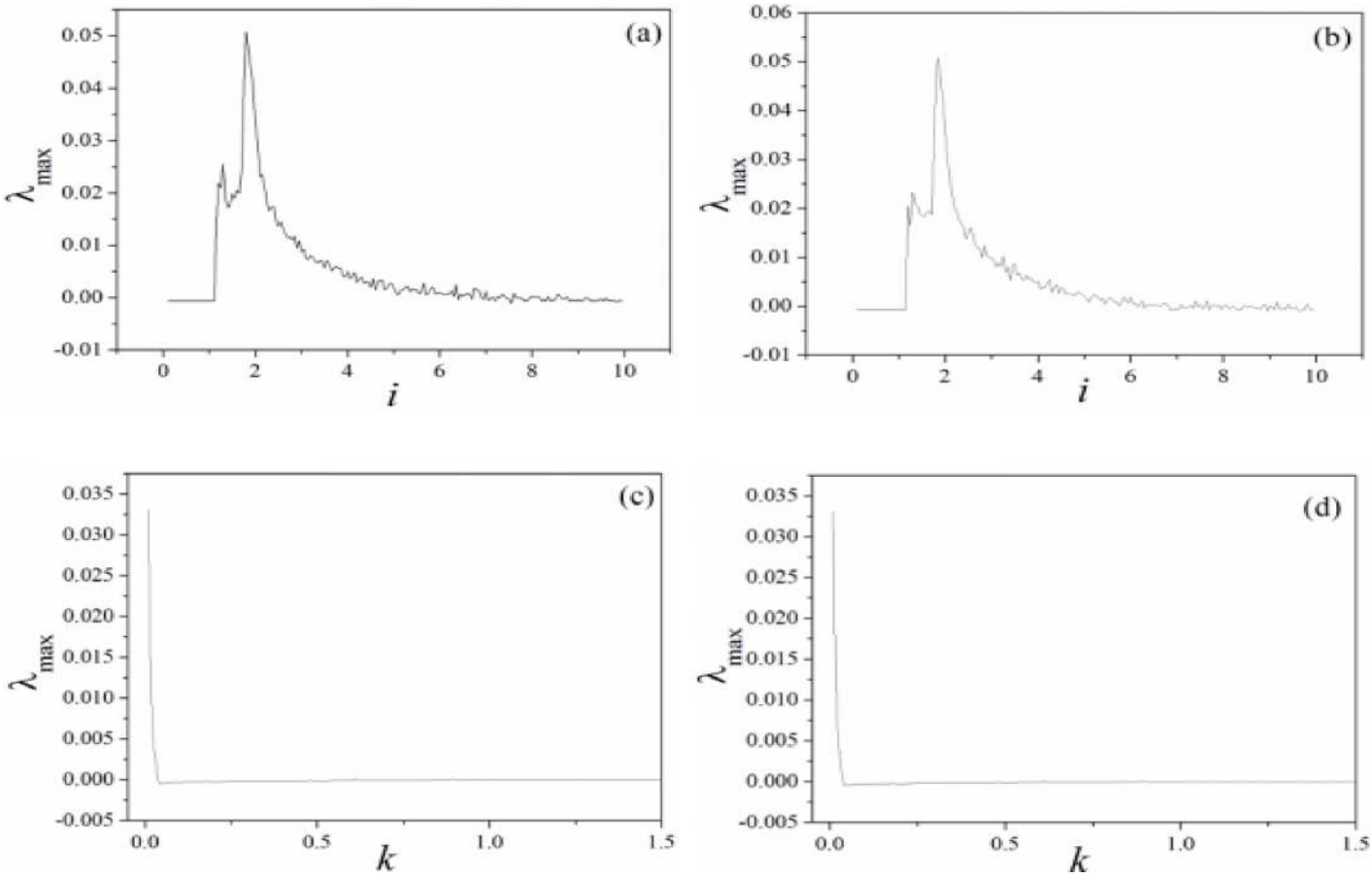

Fig 9. Distribution for largest Lyapunov exponent spectrum is calculated by changing the bifurcation parameter. (a)$\alpha = 0.1$, $\beta = 0.01$, $k = 0.01$; b)$\alpha = 4$, $\beta = 0.01$, $k = 0.01$; c)$\alpha = 0.1$, $\beta = 0.01$, $i = 1.2$; c)$\alpha = 0.1$, $\beta = 0.01$, $i = 2.0$.

https://doi.org/10.1371/journal.pone.0191120.g009

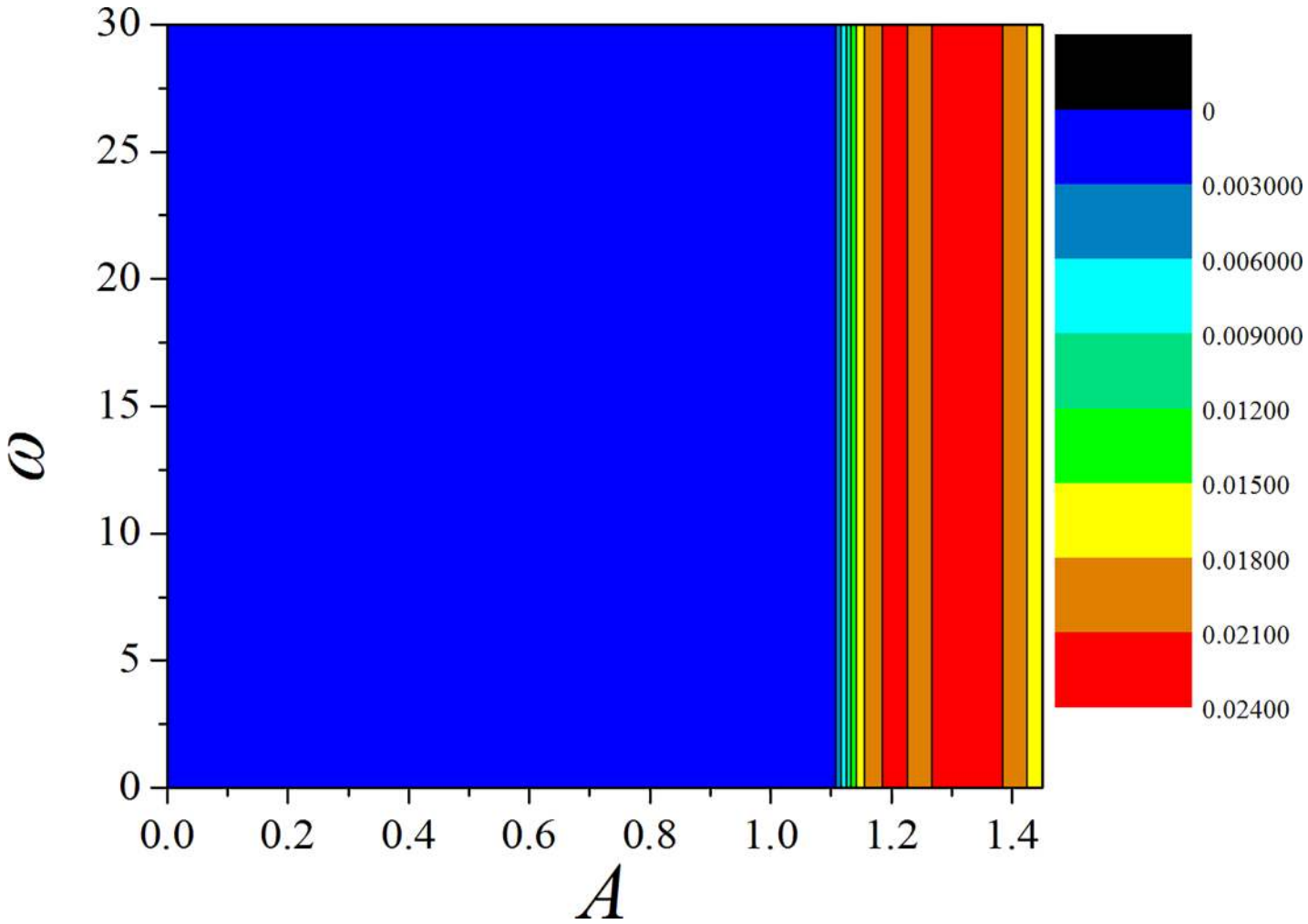

Fig 10. Distribution for largest Lyapunov exponent spectrum is calculated by applying periodical stimuli as $i = A\cos\omega t$, $k = 0.01$. The snapshots are plotted in color scale.

https://doi.org/10.1371/journal.pone.0191120.g010

junction that chaos can be controlled completely. In Fig 10, the largest Lyapunov exponent spectrum is calculated by applying different periodical stimuli on the junction.

It is confirmed that chaos can be induced by appropriate periodical stimuli when the feedback on memristor is weak. By further increasing the feedback gain in memristor, the chaos can be suppressed completely. It is important to investigate the same case on the chaotic Jerk circuit [80,81] composed of multi-scroll attractors. The dynamical equations are described by

$$\begin{cases} \dot{x} = y \\ \dot{y} = z \\ \dot{z} = -ay - az + a\sin 2\pi bx \end{cases}; \tag{11}$$

As confirmed in Ref.[82], the Jerk circuit shown in Eq (11) can find chaotic behavior by setting $a = 0.3$, b = 0.25, and the number of scroll attractors is dependent on the calculating time. As a result, more scroll attractors can be generated by increasing the calculating time. In Ref. [82], Heaviside function is used to control the number selection of scroll attractors, and the result was also verified on the PSpice tool. With the similar scheme mentioned above, the

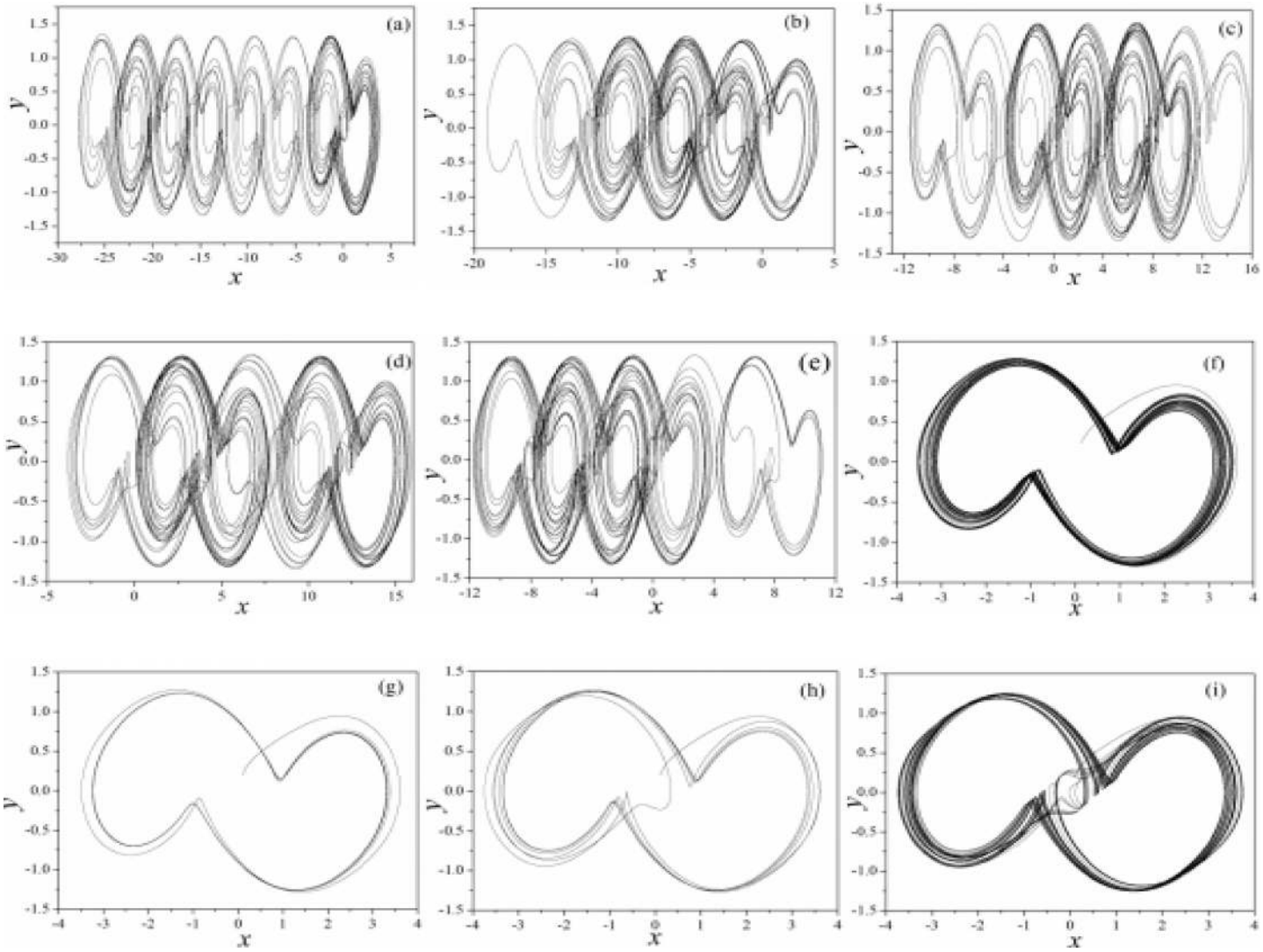

Fig 11. Selection of multi-attractor in the memristor-coupled-Jerk circuit. (a)$k = 0$, (b)$k = 0.01$, (c) $k = 0.02$, (d)$k = 0.05$, (e)$k = 0.1$, (f)$k = 0.2$, (g)$k = 0.3$, (h)$k = 0.4$, (i) $k = 0.5$. Parameters are selected as $\rho(\varphi) = 0.1+0.03\varphi^2$, $a = 0.3$, b = 0.25 and the calculating time is 1200 time units. The modulation is realized on the third variable.

https://doi.org/10.1371/journal.pone.0191120.g011

memristor-coupled Jerk circuit can be described by

$$\begin{cases} \dot{x} = y \\ \dot{y} = z \\ \dot{z} = -ay - az + a\sin 2\pi bx - k\rho(\varphi)z \\ \dot{\varphi} = kz \end{cases}; \tag{12}$$

where the term $\rho(\varphi)$ represents the same meaning in Eq (6), as a result, the Eq (12) is reduced to the Jerk circuit as shown in Eq (11) when the effect of memristor is removed. To be consistent with the previous assumption, parameters are selected as $a = 0.3$, $b = 0.25$, and the feedback gain k is changed to stabilize the multi-scroll attractors. According to Eq (12), multi-scroll attractors are calculated in Fig 11 by selecting appropriate parameter k.

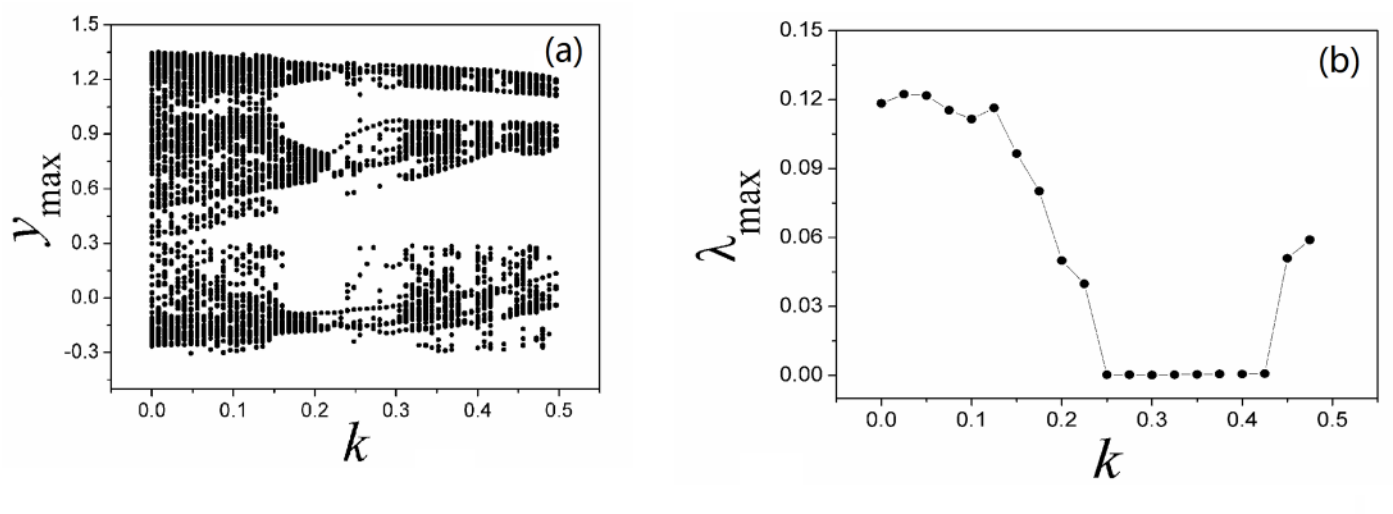

Fig 12. Bifurcation diagram (a) and Largest Lyapunov diagram (b) are calculated by changing the coefficient *k*. The parameters are selected as $\alpha = 0.1$, $\beta = 0.01$, $i = 1.2$, $a = 0.3$, $b = 0.25$ for Eq (12). y_{max} is the maximal value of sampled time series for variable y.

https://doi.org/10.1371/journal.pone.0191120.g012

It is confirmed that different numbers of scroll attractors can be selected by applying appropriate feedback gain in memristor, and extensive numerical investigations find that appropriate feedback gain can be found to select the required number of scroll attractors even the calculating period is increased. With the similar scheme, sampled time series are calculated to find the largest Lyapunov exponent and bifurcation stability, the results are shown in Fig 12.

Compared the results in Fig 12 with Fig 8, the bifurcation diagram becomes more abundant and the evolution of largest Lyapunov exponent shows distinct transmission to predict the occurrence of chaos to periodicity to chaos. As presented in Eq (12), memristor function and magnetic variable are used, and the dynamical behaviors could be dependent on the initial setting as well. In Fig 13, the dependence of initial setting is detected.

The results in Fig 13 confirmed that the improved Jerk circuit shown in Eq (12) is also much dependent on the initial values, and it is helpful to trigger and form different attractors by resetting the initial values for magnetic flux. We also investigated the case when memristor modulation is applied on the second variable, it reads as follows

$$\begin{cases} \dot{x} = y \\ \dot{y} = z - k\rho(\varphi)y \\ \dot{z} = -ay - az + a\sin 2\pi bx \\ \dot{\varphi} = ky \end{cases}; \tag{13}$$

where the parameters are used the same for Eq (12), the results are calculated in Fig 14.

As confirmed in Fig 14, the multi-scroll attractors can be stabilized from infinite number of scroll attractors by applying appropriate feedback on the Jerk circuit. That is to say, the memristor coupling on the Jerk circuit is effective to control the multi-scroll attractors completely. Furthermore, the bifurcation analysis and initials dependence are calculated. In Fig 15, sampled time series for variable are produced to find bifurcation transition and the largest Lyapunov exponent for Eq (13).

As confirmed in Fig 15, the maximal value for the variable is modulated greatly and the bifurcation sounds like anti-double periodical bifurcation with increasing the feedback coefficient k, and the largest Lyapunov exponent is decreased greatly. As a result, continuous

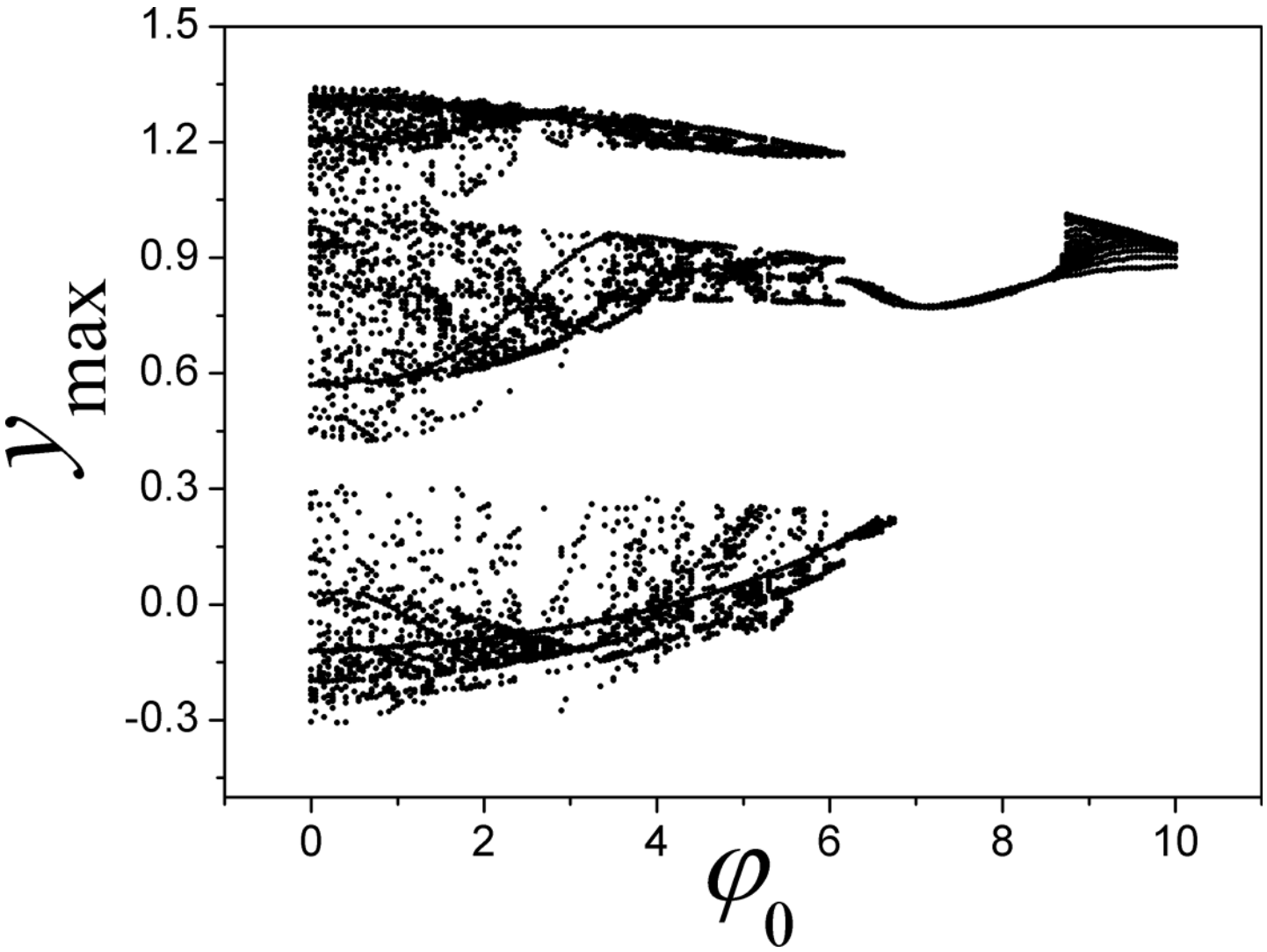

Fig 13. Bifurcation diagram is calculated for maximal state variable y_{max} vs the parameter φ_0. The parameters are selected as $\alpha = 0.1$, $\beta = 0.01$, $a = 0.3$, $b = 0.25$, $k = 0.1$ for Eq (12).

https://doi.org/10.1371/journal.pone.0191120.g013

decreasing for a larger feedback coefficient k could trigger double periodical bifurcation and chaos is generated. We also checked the initials dependence for Eq (13), and the results are presented in Fig 16.

That is, the outputs and the attractors are much dependent on the initial values for variable magnetic flux. As a result, it provides an effective way to select appropriate attractor and orbits by setting appropriate initial values for variable magnetic flux.

In fact, the modulation from memristor can impose nonlinear negative feedback on the dynamical system, thus the outputs can be adjusted carefully. This scheme can be further used to control chaos, hyperchaos in other dynamical systems. For readers' interests, these results can be further verified on PSpice and experimental circuits. It is also important to clarify some relevant questions for dynamical analysis. The algorithm proposed by Wolf [83] could be effective to estimate the possibility for occurrence of chaos by calculating the Lyapunov exponents with long period series and positive Lyapunov exponent seems to be effective to give evidence for emergence of chaos for most of dynamical systems. Maybe, finite-time local Lyapunov

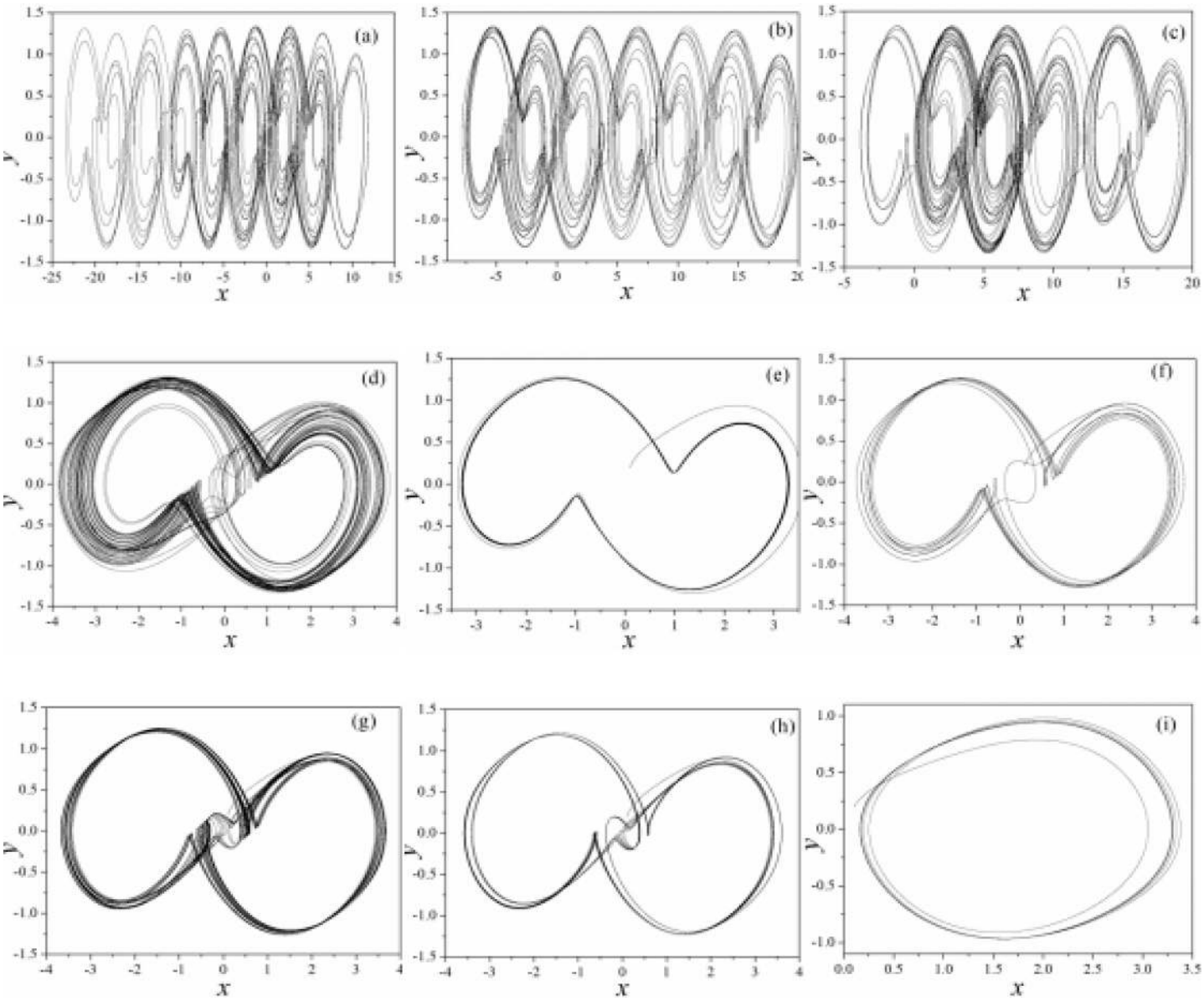

Fig 14. Selection of multi-attractor in the memristor-coupled-Jerk circuit. (a)k = 0.01, (b)k = 0.02, (c) k = 0.05, (d)k = 0.1, (e)k = 0.2, (f)k = 0.3, (g)k = 0.4, (h)k = 0.5, (i) k = 1.0. Parameters are selected as $\rho(\varphi) = 0.1+0.03\varphi^2$, a = 0.3, b = 0.25 and the calculating time is 1200 time units. The modulation is realized on the second variable.

https://doi.org/10.1371/journal.pone.0191120.g014

exponents spectrum and finite-time local Lyapunov exponent could be more appreciated since LEs were computed along one considered trajectory and for a finite-time. If LEs are the same for any initial point in the phase space, then Kaplan and Yorke suggested to call them "absolute" (see Frederickson et all 1983, page 190) and wrote that such absolute values rarely exist (thus a local LEs computed along one specific trajectory may not characterize the behaviour of the system for all initial data, especially in the case of multistability. For example, when memristor is considered, the effect of initial setting becomes more important. Therefore, the dynamical analysis for Eq (6) is worthy of further investigating, and readers can find useful scheme guidance in Refs.[84,85].

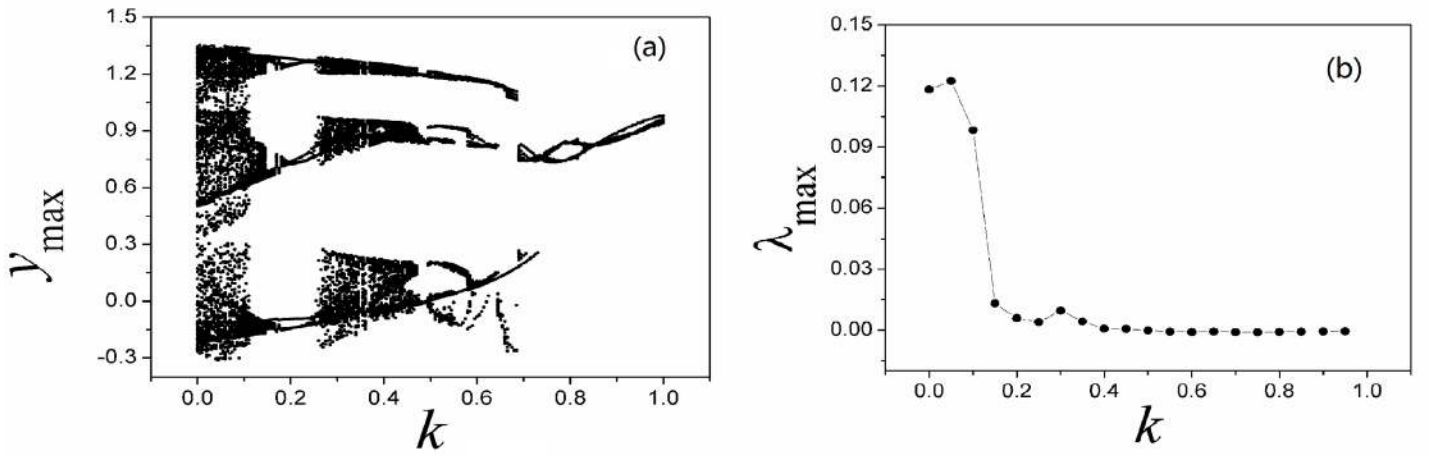

Fig 15. Bifurcation diagram (a) and Largest Lyapunov diagram (b) are calculated by changing the coefficient *k*. The parameters are selected as $\alpha = 0.1$, $\beta = 0.01$, $i = 1.2$, $a = 0.3$, $b = 0.25$ for Eq (13). y_{max} is the maximal value of sampled time series for variable y.

https://doi.org/10.1371/journal.pone.0191120.g015

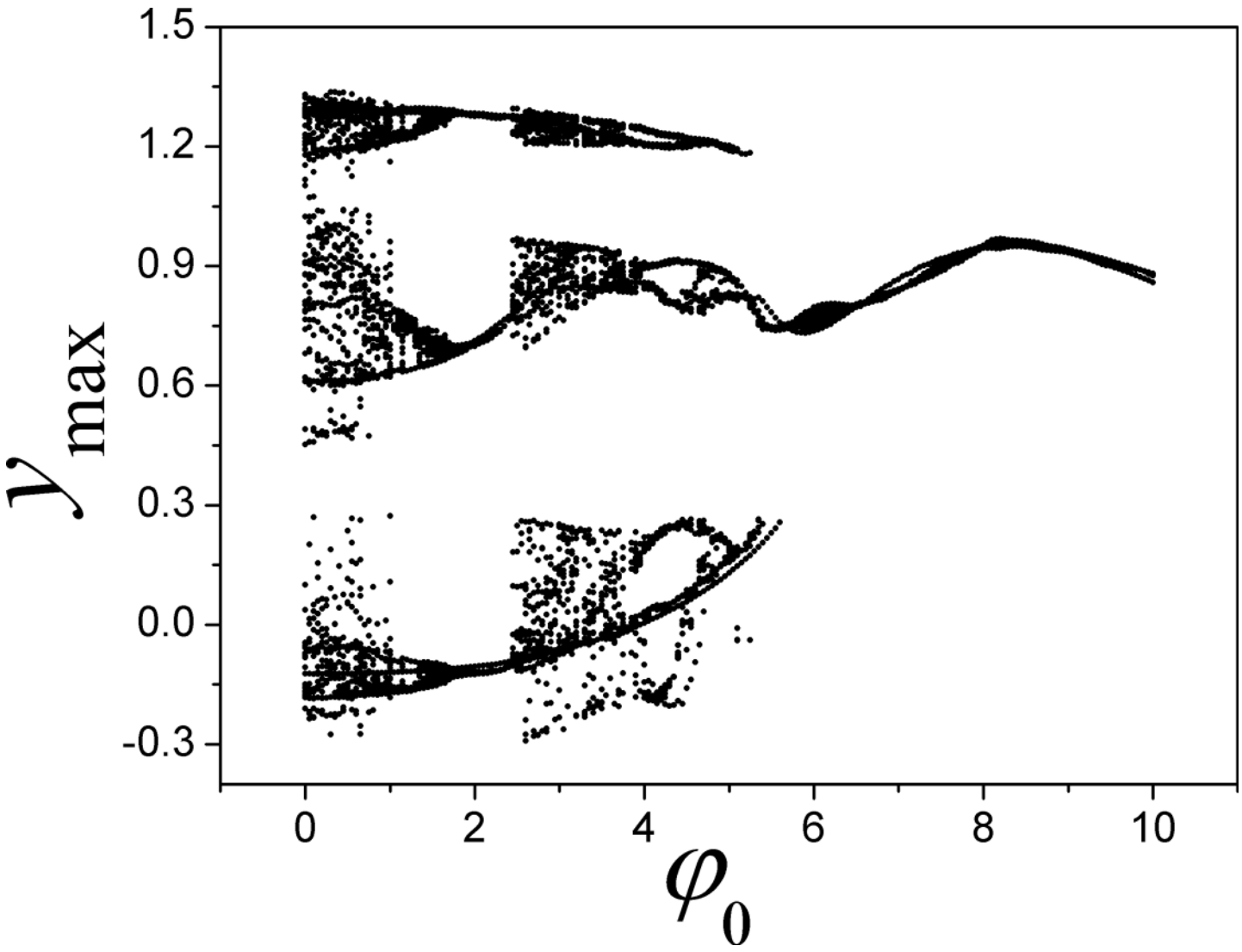

Fig 16. Bifurcation diagram is calculated for maximal state variable y_{max} vs the parameter φ_0. The parameters are selected as $\alpha = 0.1$, $\beta = 0.01$, $a = 0.3$, $b = 0.25$, $k = 0.1$ for Eq (13).

https://doi.org/10.1371/journal.pone.0191120.g016

Conclusions

In this paper, memristor is used to control the chaotic behaviors in a RCL-shunted Junction circuit by imposing induction current generated from memristor. The extended and improved four-variable dynamical system can be controlled by the coupling intensity (or feedback gain) between the memristor and the RCL-shunted junction circuit. The effect of external stimuli is discussed as well. Furthermore, this problem is also verified to control multi-scroll attractors in jerk circuit, and it is found that finite number of attractors can be stabilized from the infinite number of scroll-attractors by applying appropriate feedback gain in memristor coupled with the jerk circuit. As a result, this scheme can be further used to suppress (or enhance, positive feedback type) chaotic behaviors in other nonlinear dynamical systems driven by memristor, which is also effective to bridge two neurons and then the synchronization approach can be controlled[86–88].

Supporting information

S1 File. The data for contour plot of largest Lyapunov exponent spectrum(shown in Fig 10).
(DAT)

Acknowledgments

This project is partially supported by National Natural Science Foundation of China under Grant Nos. 11672122 and 11365014. The funders have no role in study design, data collection and analysis, decision to publish, or preparation of the manuscript.

Author Contributions

Data curation: Jun Ma, Chunni Wang.

Formal analysis: Jun Ma, Ping Zhou, Bashir Ahmad, Guodong Ren, Chunni Wang.

Project administration: Chunni Wang.

Writing – original draft: Jun Ma.

Writing – review & editing: Jun Ma.

References

1. Nakagawa M. Chaos and Fractal Properties of EEG Data, Chaos and Fractals in Engineering. 1999; pp. 113–146.
2. Correia M J, Rech P C. Hyperchaos in a new four dimensional autononmous system. International Journal of Bifurcation and Chaos. 2010; 20: 2395.
3. Savi M A, Pacheco P M C L. Chaos and hyperchaos in shape memory system.International Journal of Bifurcation and Chaos. 2002; 12: 645.
4. Gambuzza L V, Fortuna L, Frasca M, Gale E. Experimental Evidence of Chaos from Memristors. International Journal of Bifurcation and Chaos. 2015; 25:1550101.
5. Yuan F, Wang G Y, Jin P P, Wang X Y, Ma G J. Chaos in a meminductor-based Circuit. International Journal of Bifurcation and Chaos. 2016; 26: 1650130.
6. Biswas D, Banerjee T. A simple chaotic and hyperchaotic time-delay system: design and electronic circuit implementation. Nonlinear Dynamics.2016; 83:2331–2347.
7. Sprott J C, A new class of chaotic circuit, Physics Letters A. 2000; 266:19–23
8. Mengue A D, Essimbi B Z. Secure communication using chaotic synchronization in mutually coupled semiconductor lasers. Nonlinear Dynamics.2012; 70:1241–1253.

9. Liu S T, Zhang F F. Complex function projective synchronization of complex chaotic system and its applications in secure communication. Nonlinear Dynamics.2014; 76:1087–1097.
10. Chen P, Yu S M, Zhang X Y, He J B, Lin Z S, Li C Q et al. ARM-embedded implementation of a video chaotic secure communication via WAN remote transmission with desirable security and frame rate. Nonlinear Dynamics. 2016; 86: 725–740.
11. Hassan M F. Synchronization of uncertain constrained hyperchaotic systems and chaos-based secure communications via a novel decomposed nonlinear stochastic estimator. Nonlinear Dynamics.2016; 83: 2183–2211.
12. Khan M. A novel image encryption scheme based on multiple chaotic S-boxes. Nonlinear Dynamics. 2015; 82: 527–533.
13. Pyragas K, Tamaševičius A. Experimental control of chaos by delayed self-controlling feedback. Physics Letters A.1993; 180:99–102.
14. Nazzal J M, Natsheh A N. Chaos control using sliding-mode theory. Chaos, Solitons & Fractals. 2007; 33: 695–702.
15. Christini D J, Collins J J. Using chaos control and tracking to suppress a pathological nonchaotic rhythm in a cardiac model. Physical Review E.1996; 53:R49.
16. Tavazoei M S, Haeri M. Chaos control via a simple fractional-order controller. Physics Letters A.2008; 372: 798–807.
17. Vincent U E, Njah A N, Laoye J A. Controlling chaos and deterministic directed transport in inertia ratchets using backstepping control. Physica D. 2007; 231:130–136.
18. Wang Y, Wang C N, Ren G D, Tang J, Jin W Y. Energy dependence on modes of electric activities of neuron driven by multi-channel signals. Nonlinear Dynamics. 2017; 89:1967–1987.
19. Ma J, Wu F Q, Jin W Y, Zhou P, Hayat T. Calculation of Hamilton energy and control of dynamical systems with different types of attractors, Chaos. 2017; 27:053108. https://doi.org/10.1063/1.4983469 PMID: 28576108
20. Tyukin I, Steur E, Nijmeijer H, Fairhurst D,Song I, Semyanov A. State and parameter estimation for canonic models of neural oscillators. International Journal of Neural Systems.2010; 20:193. https://doi.org/10.1142/S0129065710002358 PMID: 20556847
21. Fairhurst D, Tyukin I, Nijmeijer I, van Leeuwen C. Observers for Canonic Models of Neural Oscillators. Math Model Nat Phenom. 2010; 5(2):146–184.
22. Wang C N, He Y J, Ma J, Huang L. Parameters estimation, mixed synchronization, and antisynchronization in chaotic systems. Complexity. 2014; 20(1):64–73.
23. Wang C N, Ma J, Jin W Y. Identification of parameters with different orders of magnitude in chaotic systems. Dynamical Systems.2012; 27(2):253–270.
24. Ma J, Li F, Huang L, Jin W Y. Complete synchronization, phase synchronization and parameters estimation in a realistic chaotic system. Communications in Nonlinear Science and Numerical Simulation. 2011; 16:3770–3785.
25. Shi X R, Wang Z L. The alternating between complete synchronization and hybrid synchronization of hyperchaotic Lorenz system with time delay. Nonlinear Dynamics. 2012; 69:1177–1190.
26. Li D, Zhang X P. Impulsive synchronization of fractional order chaotic systems with time-delay, Neurocomputing. 2016; 216:39–44.
27. Ma J, Zhang A H, Xia Y F, Zhang L P. Optimize design of adaptive synchronization controllers and parameter observers in different hyperchaotic systems. Applied Mathematics and Computation. 2010; 215:3318–3326.
28. Mobayen S, Finite-time stabilization of a class of chaotic systems with matched and unmatched uncertainties: An LMI approach, Complexity. 2016; 21 (5): 14–19.
29. Mobayen S, Baleanu D, Tchier F. Second-order fast terminal sliding mode control design based on LMI for a class of non-linear uncertain systems and its application to chaotic systems. Journal of Vibration and Control. 2017; 23(18): 2912–2925.
30. Mobayen S, Tchier F. Synchronization of a Class of uncertain chaotic Systems with Lipschitz nonlinearities using state-feedback control design: A matrix inequality approach. Asian Journal of Control. 2017; https://doi.org/10.1002/asjc.1512
31. Mofid O, Mobayen S. Adaptive synchronization of fractional-order quadratic chaotic flows with nonhyperbolic equilibrium. Journal of Vibration and Control. 2017; https://doi.org/10.1177/1077546317740021
32. Hao Y H, Gong Y B, Lin X, Xie Y, Ma X. Transition and enhancement of synchronization by time delays in stochastic Hodgkin–Huxley neuron networks. Neurocomputing. 2010; 73:16–18.

33. Yu H T, Wang J, Liu Q X, Deng B, Wei X L. Delayed feedback control of bursting synchronization in small-world neuronal networks. Neurocomputing. 2013; 99:178–187.
34. Lü L, Li C R, Bai S Y, Gao L, Ge L, Han C. Cluster synchronization between uncertain networks with different dynamics. Physica A. 2017; 469:429–437.
35. Wang C N, Ma J. A review and guidance for pattern selection in spatiotemporal system. International Journal of Modern Physics B. 2018; 32:1830003.
36. Kondo S. An updated kernel-based Turing model for studying the mechanisms of biological pattern formation. Journal of Theoretical Biology. 2017; 414:120–127. https://doi.org/10.1016/j.jtbi.2016.11.003 PMID: 27838459
37. Camara B I, Haque M, Mokrani H. Patterns formations in a diffusive ratio-dependent predator-prey model of interacting populations. Physica A. 2016; 461:374–383.
38. Yu W T, Tang J, Ma J, Yang X. Heterogeneous delay-induced asynchrony and resonance in a small-world neuronal network system. EPL. 2016; 114:50006.
39. Ma J, Tang J. A review for dynamics of collective behaviors of network of neurons, Science China Technological Sciences. 2015; 58: 2038–2045.
40. Xiao W W, Gu H G, Liu M R. Spatiotemporal dynamics in a network composed of neurons with different excitabilities and excitatory coupling. Science China Technological Sciences. 2016; 59:1943–1952.
41. Wang G P, Jin W Y, Wang A. Synchronous firing patterns and transitions in small-world neuronal network, Nonlinear Dynamics. 2015; 81:1453–1458.
42. Ma J, Tang J. A review for dynamics in neuron and neuronal network. Nonlinear Dynamics. 2017; 89: 1569–1578.
43. Zhang Q Y, Tian C R. Pattern dynamics in a diffusive Rössler model, Nonlinear Dynamics. 2014; 78:1489–1501.
44. Zhang Q Q, Shen J W. Pattern formation in the FitzHugh-Nagumo model. Computers & Mathematics with Applications. 2015; 70: 1082–1097.
45. Bekkers J M. Synaptic transmission: Functional autapses in the cortex. Current Biology. 2003; 13: 433–435.
46. Herrmann C S. Klaus A. Autapse Turns Neuron into Oscillator. International Journal of Bifurcation and Chaos. 2004; 14: 623–633.
47. Wang H T, Wang L F, Chen Y L, Chen Y. Effect of autaptic activity on the response of a Hodgkin-Huxley neuron. Chaos. 2014; 24: 033122. https://doi.org/10.1063/1.4892769 PMID: 25273202
48. Ren G D, Wu G, Ma J, Chen Y. Simulation of electric activity of neuron by setting up a reliable neuronal circuit driven by electric autapse. Acta Physica Sinica. 2015; 64:058702(In Chinese)
49. Song X L, Wang C N, Ma J, Tang J. Transition of electric activity of neurons induced by chemical and electric autapses. Science China Technological Sciences. 2015; 58:1007–1014(2015)
50. Ma J, Song X, Jin W, Wang C. Autapse-induced synchronization in a coupled neuronal network, Chaos Solitons & Fractals. 2015; 80:31–38.
51. Ma J, Song X L, Tang J, Wang C N. Wave emitting and propagation induced by autapse in a forward feedback neuronal network. Neurocomputing. 2015; 167:378–389.
52. Ma J, Qin H X, Song X L, Chu R T. Pattern selection in neuronal network driven by electric autapses with diversity in time delays. International Journal of Modern Physics B. 2015; 29(1):1450239.
53. Wang C N, Guo S L, Xu Y, Ma J, Tang J, Alzahrani F. Formation of autapse connected to neuron and its biological function. Complexity. 2017; 2017: 5436737.
54. Kawaguchi T. Phase dynamics of a Josephson junction ladder driven by modulated currents. Physica C. 2011; 471: 21–22.
55. Machura L, Kostur M, Talkner P, Hänggi P, Łuczka J. Negative conductances of Josephson junctions: Voltage fluctuations and energetics. Physica E. 2010; 42:590–594.
56. Crotty P, Schult D, Segall K. Josephson junction simulation of neurons. Physical Review E. 2010; 82: 011914.
57. Li F, Liu Q R, Guo H Y, Zhao Y H, Tang J, Ma J. Simulating the electric activity of FitzHugh–Nagumo neuron by using Josephson junction model. Nonlinear Dynamics. 2012; 69:2169–2179.
58. Strukov D B, Snider G S, Stewart D R, Williams R S. The missing memristor found. Nature. 2008; 453 (7191): 80–83. https://doi.org/10.1038/nature06932 PMID: 18451858
59. Itoh M, Chua L O. Memristor oscillators. International Journal of Bifurcation and Chaos. 2008; 18(11): 3183–3206.

60. Muthuswamy B, Kokate P P. Memristor-based chaotic circuits. IETE Technical Review. 2009; 26 (6):417–429.
61. Zhou L, Wang C H, Zhou L L. Generating hyperchaotic multi-wing attractor in a 4D memristive circuit. Nonlinear Dynamics. 2016; 85:2653–2663.
62. Li Q D, Zeng H Z, Li J. Hyperchaos in a 4D memristive circuit with infinitely many stable equilibria. Nonlinear Dynamics. 2015; 79:2295–2308.
63. Lv M, Wang C N, Ren G D, Ma J, Song X L. Model of electrical activity in a neuron under magnetic flow effect. Nonlinear Dynamics. 2016; 85:1479–1490.
64. Lv M, Ma J. Multiple modes of electrical activities in a new neuron model under electromagnetic radiation. Neurocomputing. 2016; 205:375–381.
65. Ma J, Wu F Q, Wang C N. Synchronization behaviors of coupled neurons under electromagnetic radiation. International Journal of Modern Physics B. 2017; 31(2):1650251.
66. Wu F Q, Wang C N, Jin W Y, Ma J. Dynamical responses in a new neuron model subjected to electromagnetic induction and phase noise. Physica A. 2017; 469: 81–88.
67. Wu F Q, Wang C N, Xu Y, Ma J. Model of electrical activity in cardiac tissue under electromagnetic induction. Scientific Reports. 2016; 6:28. https://doi.org/10.1038/s41598-016-0031-2 PMID: 28442705
68. Ren G D, Xu Y, Wang C N. Synchronization behavior of coupled neuron circuits composed of memristors. Nonlinear Dynamics. 2017; 88:893–901.
69. Njah A N, Ojo K S, Adebayo G A, Obawole A O. Generalized control and synchronization of chaos in RCL-shunted Josephson junction using backstepping design. Physica C. 2010; 470:558–564.
70. Ucar A, Lonngren K E, Bai E W. Chaos synchronization in RCL-shunted Josephson junction via active control. Chaos, Solitons & Fractals. 2007; 31:105–111.
71. Whan C B, Lobb C J. Complex dynamical behavior in RCL-shunted Josephson tunnel junctions. Physical Review E. 1996; 53:405.
72. Vincent U E, Ucar A, Laoye J A, Kareem S O. Control and synchronization of chaos in RCL-shunted Josephson junction using backstepping design. Physica C. 2008; 468:374–382.
73. Wang C N, Chu R T, Ma J. Controlling a chaotic resonator by means of dynamic track control. Complexity. 2015; 21(1):370–378.
74. Yang X S, Li Q. A computer-assisted proof of chaos in Josephson junctions. Chaos Solitons & Fractals. 2006; 27: 25–30.
75. Itoh M, Chua L O. Duality of memristor circuits. International Journal of Bifurcation and Chaos. 2013; 23: 1330001.
76. Chua L O, Sbitnev V, Kim H. Hodgkin-Huxley axon is made of memristors, International Journal of Bifurcation and Chaos. 2012; 22:1230011.
77. Pogromsky A,Glad T, Nijmeijer H. On diffusion driven oscillations in coupled dynamical systems.International Journal of Bifurcation and Chaos.1999; 9:629.
78. Boichenko V A, Leonov G A, Reitmann V. Dimension theory for ordinary differential equations.(Teubner, Stuttgart, 2005).
79. Ma J, Wu F Q, Ren G D, Tang J. A class of initials-dependent dynamical systems. Applied Mathematics and Computation. 2017; 298: 65–76.
80. Sprott J C. Simple chaotic systems and circuits. American Journal of Physics.2000; 68:758.
81. Sprott J C. A new class of chaotic circuit, Physics Letters A. 2000; 266:19.
82. Ma J, Wu X Y, Chu R T, Zhang L P. Selection of multi-scroll attractors in Jerk circuits and their verification using Pspice. Nonlinear Dynamics. 2014; 76:1951–1962.
83. Wolf A, Swift J B, Swinney H L, Vastano J A. Determining Lyapunov exponents from a time series. Physica D. 1985; 16:285–317.
84. Chen G, Kuznetsov N V, Leonov G A, Mokaev T V. Hidden attractors on one path: Glukhovsky- Dolzhansky, Lorenz, and Rabinovich systems. International Journal of Bifurcation and Chaos. 2017; 27(8): 1750115.
85. Leonov G A, Kuznetsov N V, Mokaev T N. Homoclinic orbits, and self-excited and hidden attractors in a Lorenz-like system describing convective fluid motion. European Physical Journal Special Topics. 2015; 224: 1421–1458.
86. Xu Y, Jia Y, Ma J, Alsaedi A, Ahmad B. Synchronization between neurons coupled by memristor. Chaos Solitons & Fractals. 2017; 104:435–442.
87. Guo S L, Xu Y, Wang C N, Jin W Y, Hobiny A, Ma J. Collective response, synapse coupling and field coupling in neuronal network. Chaos Solitons & Fractals. 2017; 105:120–127.

88. Chen J X, Zhang H, Qiao L Y, Liang H, Sun W G. Interaction of excitable waves emitted from two defects by pulsed electric fields, Communications in Nonlinear Science and Numerical Simulation 54 202–209(2018).